Electronic Supplementary Information (ESI)

All-PEGylated Redox-Active Metal-Free Organic Molecules for Non-Aqueous Redox Flow Battery

Jingchao Chai, Amir Lashgari, Xiao Wang, Caroline K. Williams, Jianbing "Jimmy" Jiang*

Department of Chemistry, University of Cincinnati, P.O. Box 210172, Cincinnati, Ohio 45221-0172, United States.

*Corresponding author: jianbing.jiang@uc.edu

Table of Contents

Synthesis of compound PEG12-PTZ. A sample of NaH (2.0 g, 50 mmol, 5.0 eq) was added to the solution of phenothiazine (2.0 g, 10 mmol, 1.0 eq) in DMF (8.0 mL) and stirred at room temperature for 1 hour. Then, PEG12-OTs (5.9 g, 9.0 mmol, 0.9 eq) was added to the reaction mixture and continued stirring at room temperature for 24 hours. Water was carefully added dropwise to the residue to quench the reaction. The crude reaction mixture was washed three times with brine and extracted with ethyl acetate to remove DMF. The organic extract was combined and dried over Na_2SO_4. The solution was filtered, and the filtrate was dried via rotavate. The crude residue was purified by column chromatography (SiO_2; 10% MeOH in CH_2Cl_2) to afford the title compounds as a red oil. Yield: 4.9 g, 66%. ^{1}H NMR (400 MHz, $CDCl_3$), δ 3.37 (s, 3H), 3.39–3.76 (m, 44H), 3.78–3.89 (t, 2H, *J* = 8.0 Hz), 4.04–4.11 (t, 2H, *J* = 8.0 Hz), 6.83–6.99 (m, 4H), 7.07–7.21 (m, 4H); ^{13}C NMR (100 MHz, $CDCl_3$), δ 47.45, 59.07, 68.18, 71.86, 114.99, 122.60, 124.45, 127.35, 144.91; HR-MS obsd 764.3687, calcd 764.3650 ($[M + Na]^+$, M = $C_{37}H_{59}NO_{12}S$); Elemental analysis calcd for $C_{37}H_{59}NO_{12}S$: C, 59.90; H, 8.02; N, 1.89. Found: C, 61.25; H, 7.62; N, 2.53.

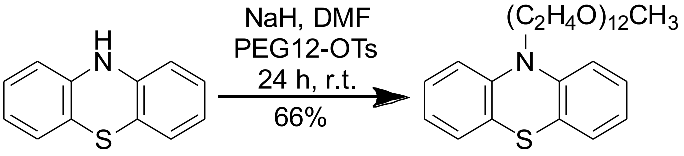

PEG12-PTZ

Scheme S1 Synthesis of compound **PEG12-PTZ**.

Synthesis of compound C3-PTZ. A sample of KOH (2.2 g, 39 mmol, 1.5 eq) was added to the solution of penothiazine (5.2 g, 26 mmol, 1.0 eq) in DMSO (60 mL) and stirred for 1 h at 40 ºC. Then, 1-iodopropane (3.1 mL, 31 mmol, 1.2 eq) was added to the mixture and stirred for 12 h at 80 ºC. The solution was washed three times with brine and extracted with ethyl acetate to remove DMSO. The organic extract was combined and dried over Na_2SO_4. The solution was filtered, and the filtrate was dried via rotavape. The crude residue was purified by column chromatography (SiO_2; hexanes) to afford the title compounds as a white solid. Yield: 4.2 g, 68%. ^{1}H NMR (400 MHz, CDCl3), δ 0.988–1.08 (t, 3H, *J* = 8 Hz), 1.79–1.94 (m, 2H), 3.74–3.92 (m, 2H), 6.81–6.99 (m, 4H), 7.09–7.24 (m, 4H); ^{13}C NMR (100 MHz, $CDCl_3$), δ 11.50, 20.22, 49.21, 115.59, 122.44, 125.01, 127.29, 127.50, 145.41; HR-MS obsd 241.0918, calcd 241.0920 (M^+, M = $C_{15}H_{15}NS$).

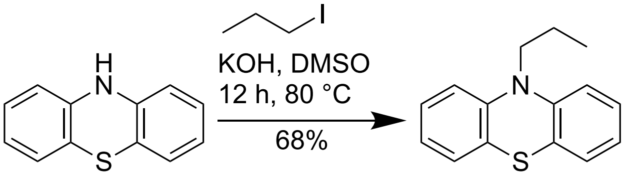

C3-PTZ

Scheme S2 Synthesis of compound **C3-PTZ**.

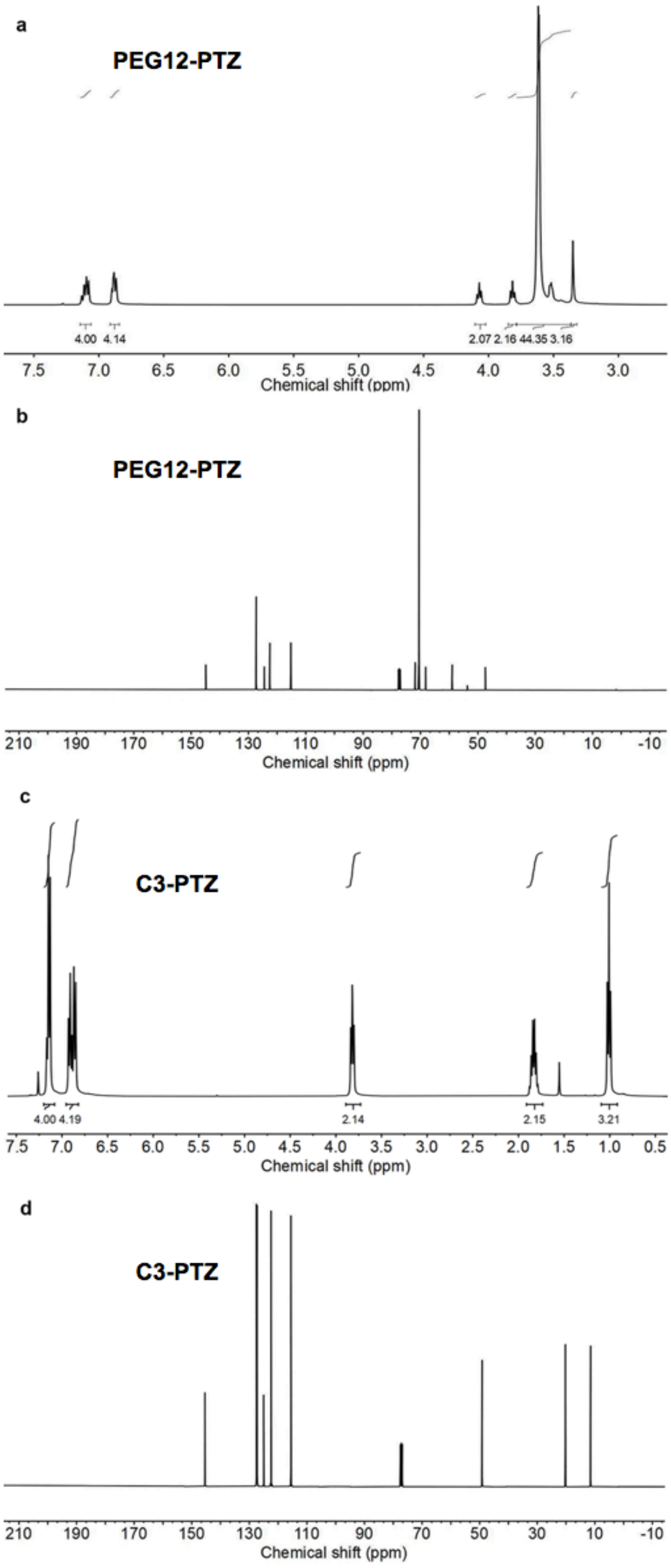

Fig. S1 ^{1}H NMR (a and c) and ^{13}C NMR (b and d) spectra of **PEG12-PTZ** and **C3-PTZ** in $CDCl_3$.

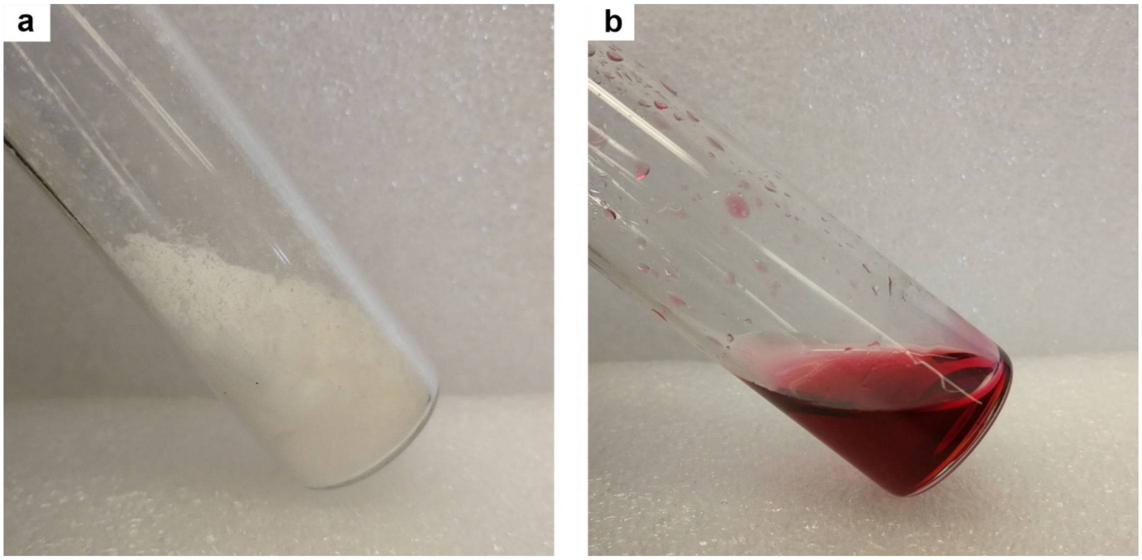

Fig. S2 Photographs of compounds **C3-PTZ** (a) and **PEG12-PTZ** (b).

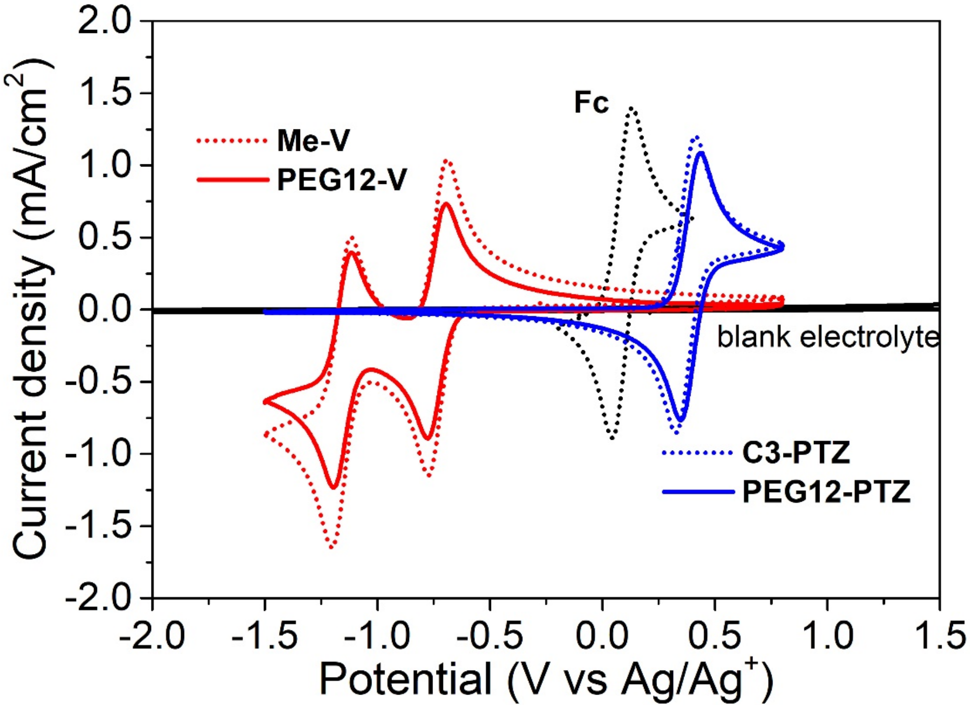

Fig. S3 CV scans of blank electrolyte, and 5 mM of **Fc**, **Me-V**, **PEG12-V**, **C3-PTZ**, and **PEG12-PTZ** in 0.1 M TBAPF$_6$-ACN. Scan rate: 50 mV/s.

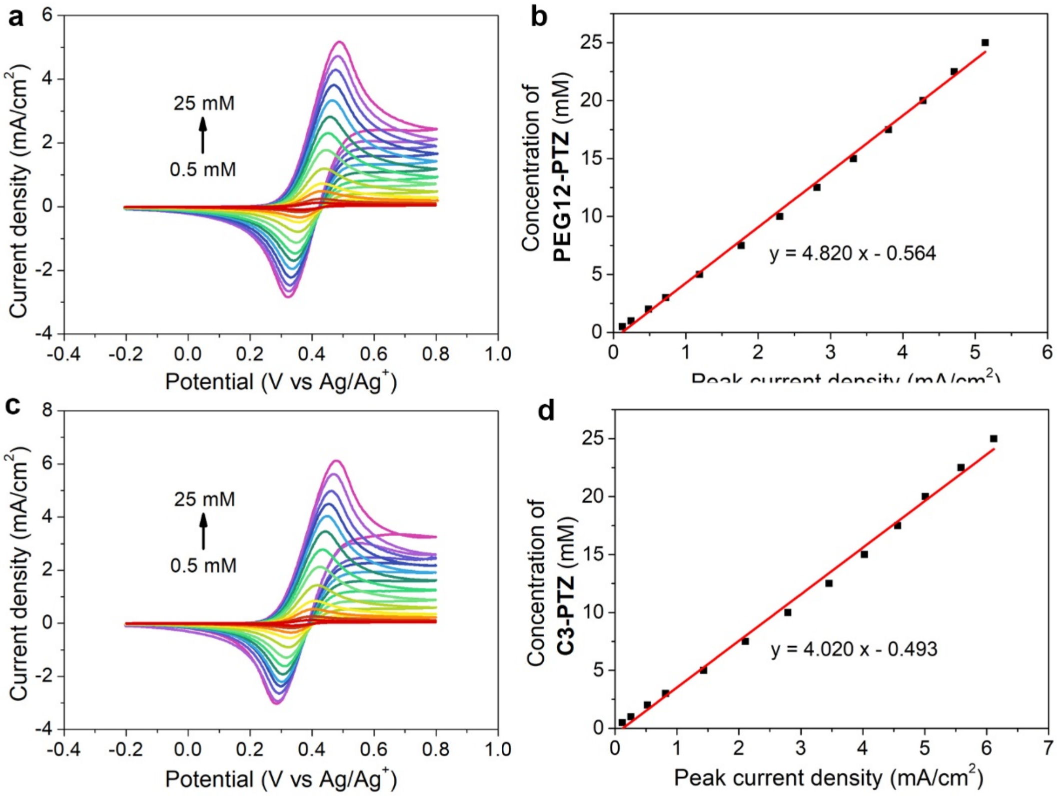

Fig. S4 CV scans of **PEG12-PTZ** (a) and **C3-PTZ** (c) at various concentrations in 0.1 M TBAPF$_6$-ACN. The relationship between concentration and oxidized peak current of **PEG12-PTZ** (b) and **C3-PTZ** (d).

Permeabilities of **C3-PTZ** or **PEG12-PTZ** were tested in a H-cell. The samples of 15 mL 0.1 M $TBAPF_6$-ACN with 50 mM **C3-PTZ** or **PEG12-PTZ** were added to one side and 0.1 M $TBAPF_6$-ACN without active materials was added in the other side. Both sides were continuously stirred on a magnetic stirrer. The CV scans of blank electrolyte over time were conducted to obtain the concentration of **C3-PTZ** and **PEG12-PTZ**. The permeability is calculated based on the following equation:[S1]

$$P = \frac{\ln\left(1 - \frac{2C_r}{C_0}\right)\left(-\frac{Vl}{2A}\right)}{t},$$

where C_r is the concentration measured at the blank electrolytes, C_0 is the original active species concentration, V is the volume (15 mL), l is the membrane thickness (4.7×10^{-4} cm), A is the membrane area (0.64 cm^2), and t is the test time.

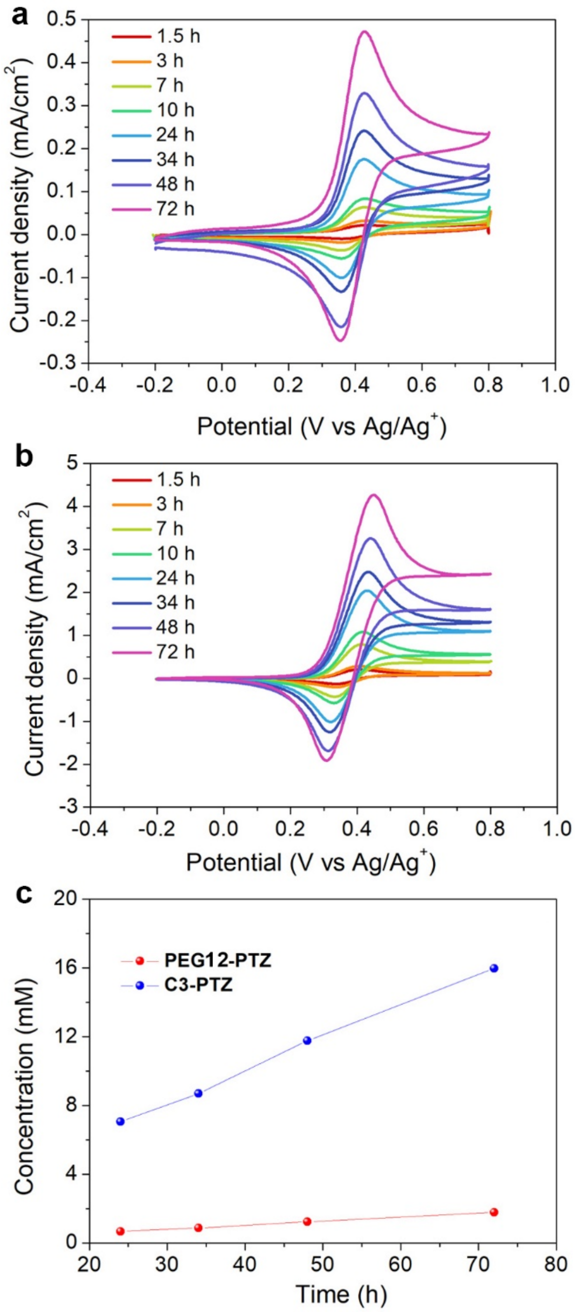

Fig. S5 Permeability test of **PEG12-PTZ** and **C3-PTZ**. CV scans of **PEG12-PTZ** (a) and **C3-PTZ** (b) in control cell over time. (c) Concentration of **PEG12-PTZ** and **C3-PTZ** in control cell. The date was calculated from Fig. S4.

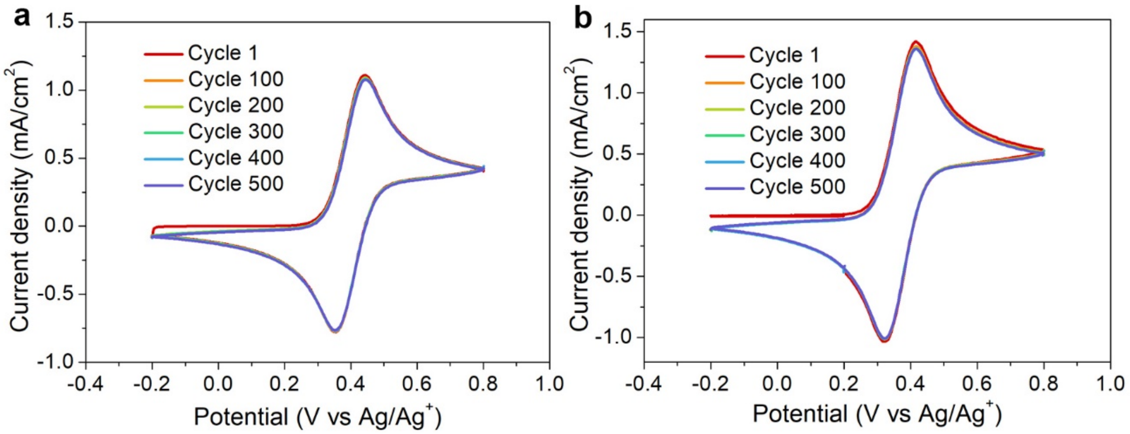

Fig. S6 Repetitive CV scans of 5 mM of **PEG12-PTZ** (a) and **C3-PTZ** (b) in 0.1 M TBAPF$_6$-ACN for 500 cycles.

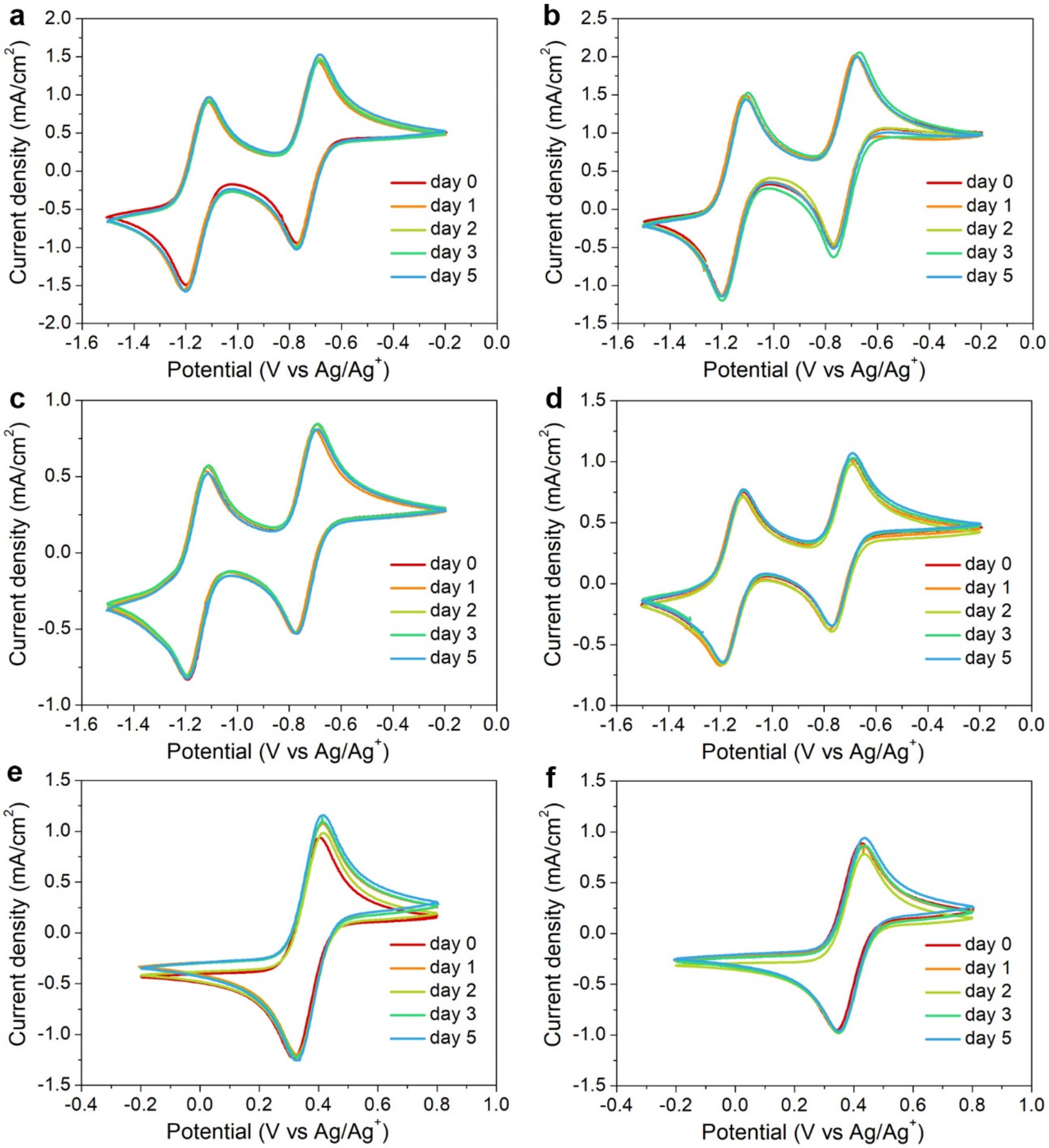

Fig. S7 CV scans of (a) (**Me-V**)$^{2-}$, (b) (**Me-V**)$^{1-}$, (c) (**PEG12-V**)$^{2-}$, (d) (**PEG12-V**)$^{1-}$, (e) (**C3-PTZ**)$^{1+}$, and (f) (**PEG12-PTZ**)$^{1+}$. The samples were tested on day 0, and after 24 h (day 1), 48 h (day 2), 72 h (day 3), 96 h (day 4), and 120 h (day 5).

The electrochemical kinetics of **PEG12-PTZ** (Fig. S8a) and **C3-PTZ** (Fig. S8c) was also investigated by CV at different scan rates ranging from 5 to 2,000 mV/s. The redox peak currents increased with scan rate and were linearly related to the square root of the scan rate, meaning that the redox reaction is diffusion-controlled. The diffusion coefficient of **PEG12-PTZ** in TBAPF$_6$-ACN was calculated from the Randle-Sevcik equation:[S2,3]

$$i_p = 0.4463\ nFAC\ (\frac{nFD\nu}{RT})^{1/2}$$

where i_p is current maximum in amps, n is number of electrons transferred (n = 1), A is electrode area (0.071 cm^2), F is Faraday Constant (96,485 C/mol), D is diffusion coefficient in cm^2/s, C is concentration in mol/cm^3 ($C = 5 \times 10^{-6}$ mol/cm^3), ν is scan rate in V/s, R is gas constant (R = 8.314 J/(K mol)) and T was temperature (298 K).

The calculated diffusion coefficients of oxidation (D_O) and reduction (D_R) process of **PEG12-PTZ/PEG12-PTZ$^+$** in TBAPF$_6$-ACN were 10.96×10^{-6} cm^2/s and $D_R = 9.88 \times 10^{-6}$ cm^2/s, respectively (Fig. S8b), slightly lower than them of **C3-PTZ/C3-PTZ$^+$** ($D_O = 16.79 \times 10^{-6}$ cm^2/s and $D_R = 16.93 \times 10^{-6}$ cm^2/s) (Fig. S8d). The reduced diffusion coefficients of **PEG12-PTZ/PEG12-PTZ$^+$** were probably due to the increase in viscosity caused by PEG chains.

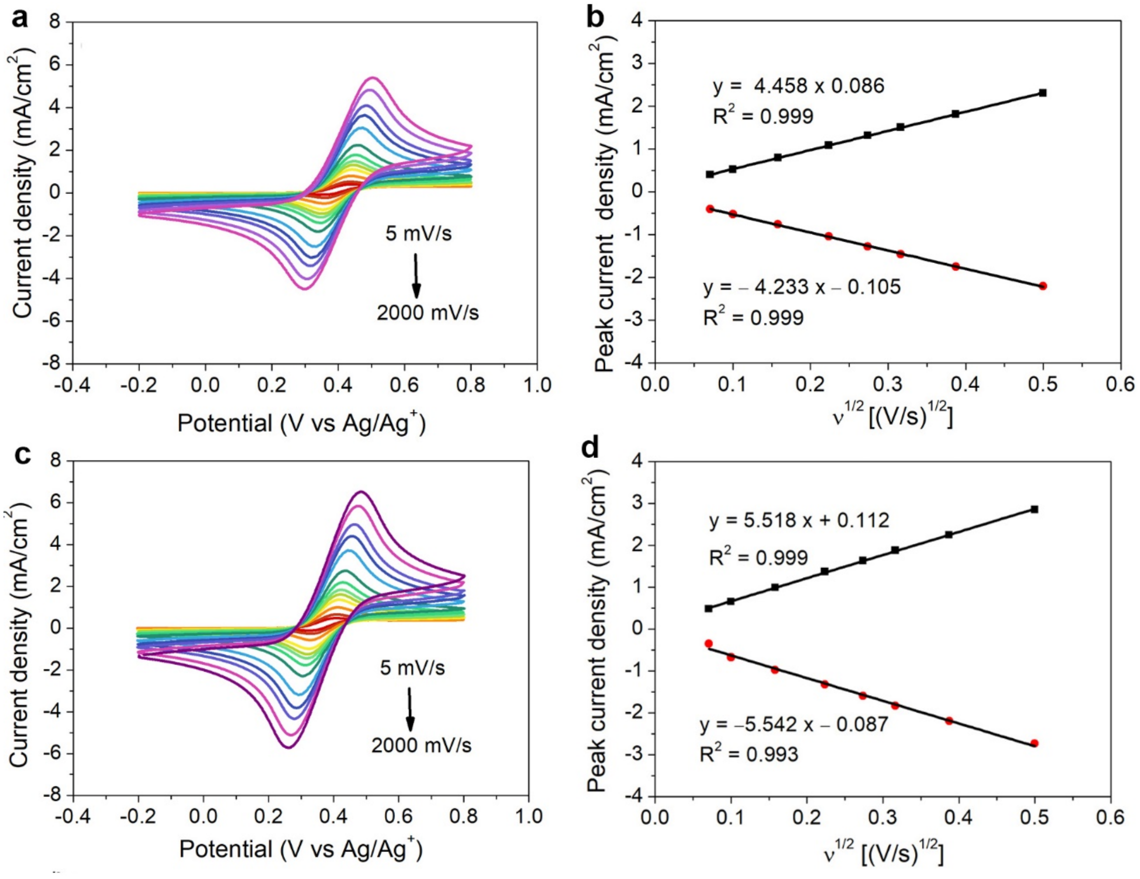

Fig. S8 CV scans of 5 mM **PEG12-PTZ** (a) and **C3-PTZ** (c) at different scan rates. Peak oxidation and reduction current densities of **PEG12-PTZ** (b) and **C3-PTZ** (d) at different scan rates.

Diffusion coefficient (D) of **PTZ**s can be calculated from Levich plot (limiting current vs $\omega^{1/2}$):[S4-6] $i_L = 0.62\ nFAD^{2/3}\omega^{1/2}\upsilon^{-1/6}C_0$, where i_L is limit current density, n is number of transferred electrons (n = 1), F is Faraday's constant (F = 96,485 C/mol), A is the surface area of the RDE (A = 0.196 cm^2), ω is the rotation speed (rad/s), υ is kinematic viscosity of 0.1 M $TBAPF_6$-ACN (υ = 0.00442 cm^2/s) and C_0 is the concentration (C_0 = 1 mM).

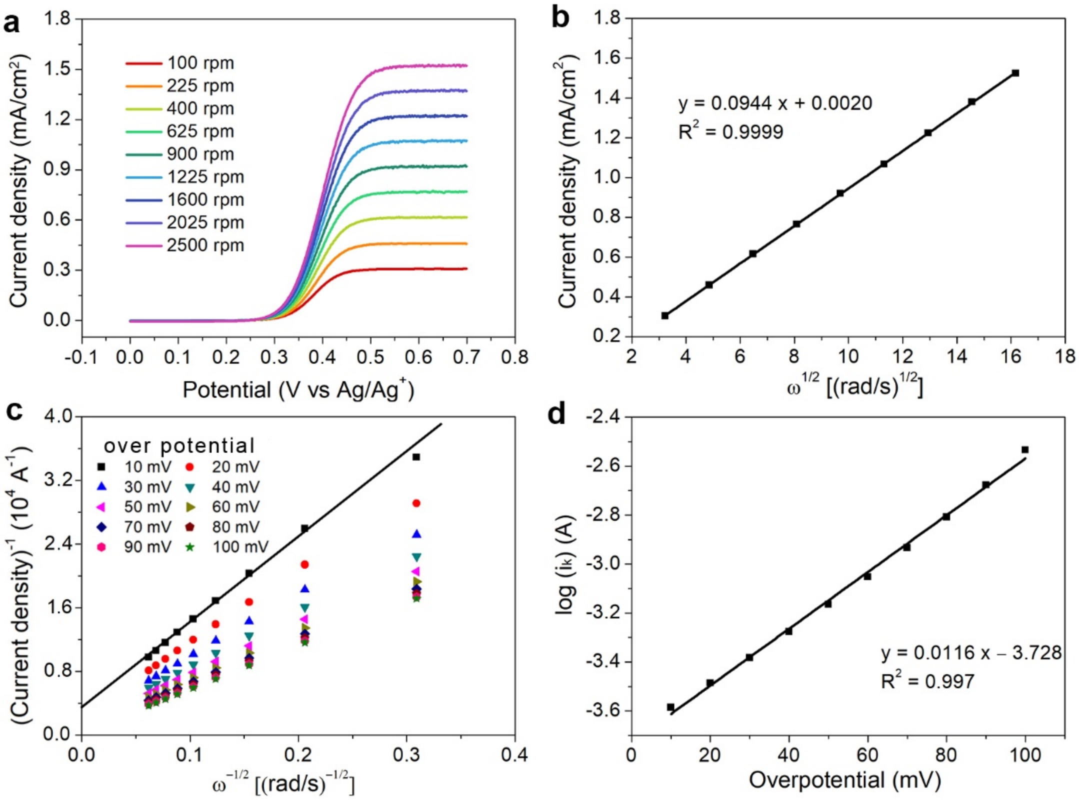

Fig. S9 (a) Linear sweep voltammetry of 1 mM **C3-PTZ** in 0.1 M TBAPF6-ACN at different rotation speeds from 100 to 2,500 rpm. (b) Levich plot from the obtained limiting currents. (c) Koutecký-Levich plot (i^{-1} vs $\omega^{-1/2}$) of 1 mM **C3-PTZ**. (d) Plot of log (i_k) vs overpotential.

Table S1 Diffusion coefficient (D) from Levich plot, diffusion coefficient (D_O and D_R) from Randle-Sevcik equation, reaction rate constant (k_0) and transfer coefficient (α) of **C3-PTZ** and **PEG12-PTZ** in 0.1 M $TBAPF_6$-ACN.

Compound	D (cm^2/s)	D_O (cm^2/s)	D_R (cm^2/s)	k_0 (cm/s)	α
C3-PTZ	1.61×10^{-5}	1.68×10^{-5}	1.71×10^{-5}	9.88×10^{-3}	0.315
PEG-PTZ	1.23×10^{-5}	1.10×10^{-5}	9.88×10^{-6}	5.64×10^{-3}	0.492

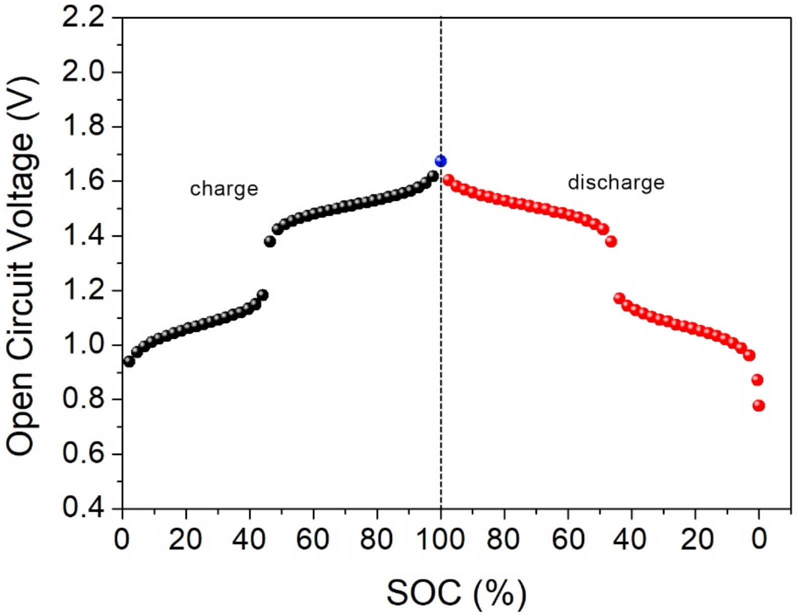

Fig. S10 OCV of the **PEG12-PTZ/PEG12-V** battery at various SOCs.

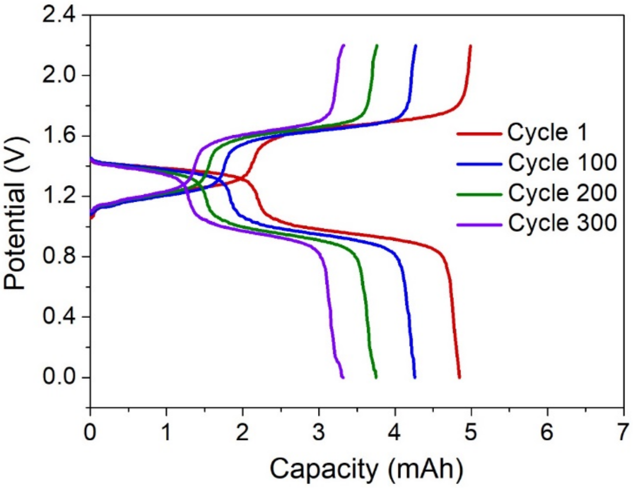

Fig. S11 Charge-discharge plots of the **PEG12-PTZ/PEG12-V** battery at different cycle numbers.

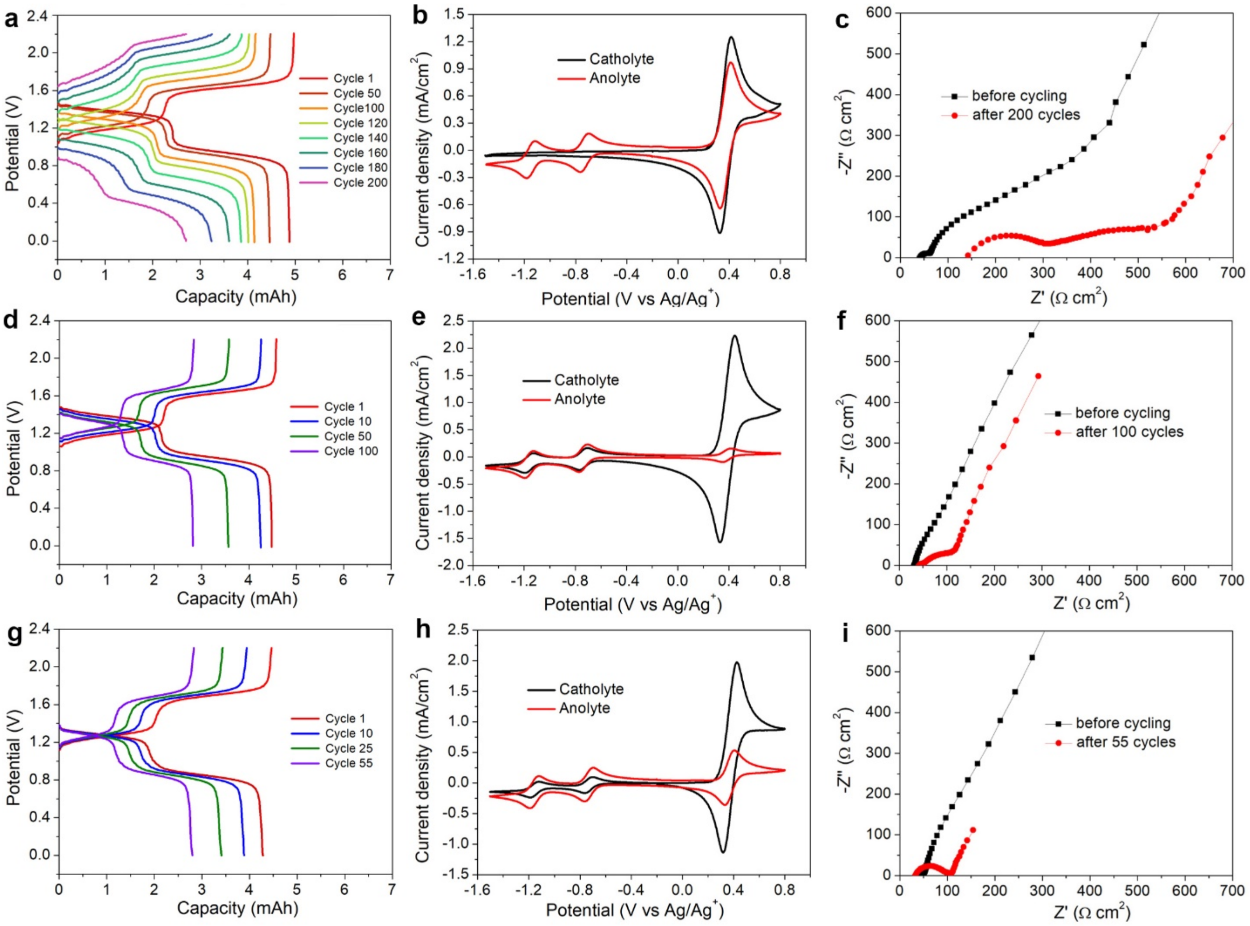

Fig. S12 The performance characterization of (a–c) **C3-PTZ/PEG-V**, (d–f) **PEG-PTZ/Me-V**, and (g–i) **C3-PTZ/Me-V** batteries. Charge-discharge curves at different cycles (a, d and g), CV scans of electrolyte after cycling (b, e and h) and AC impedance spectra (c, f and i).

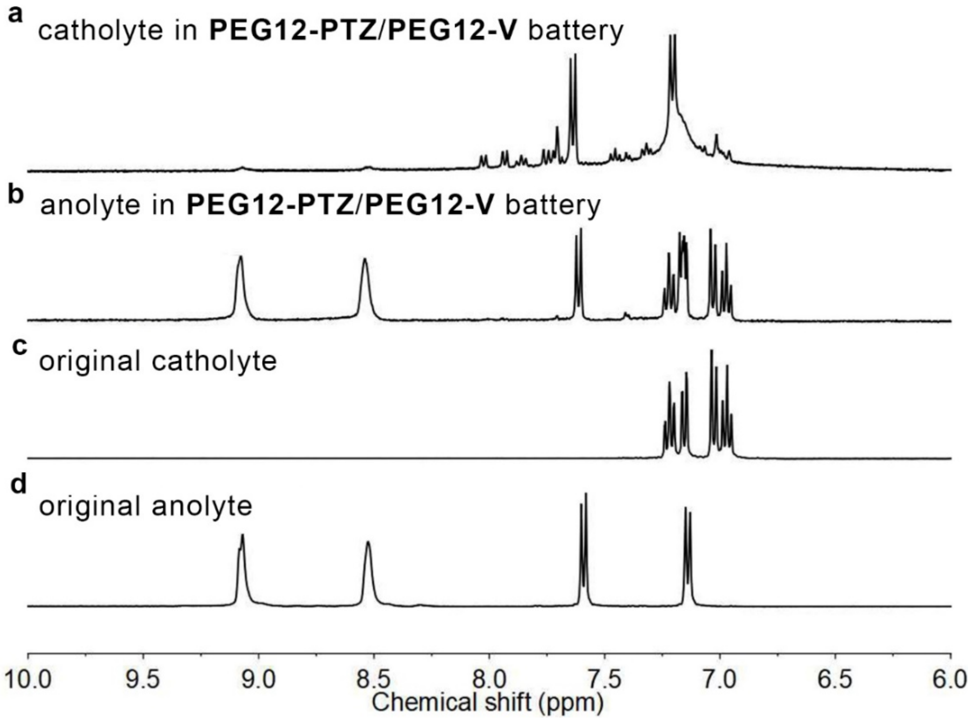

Fig. S13 ^{1}H NMR of catholyte and anolyte in **PEG12-PTZ/PEG12-V** battery before and after cycling.

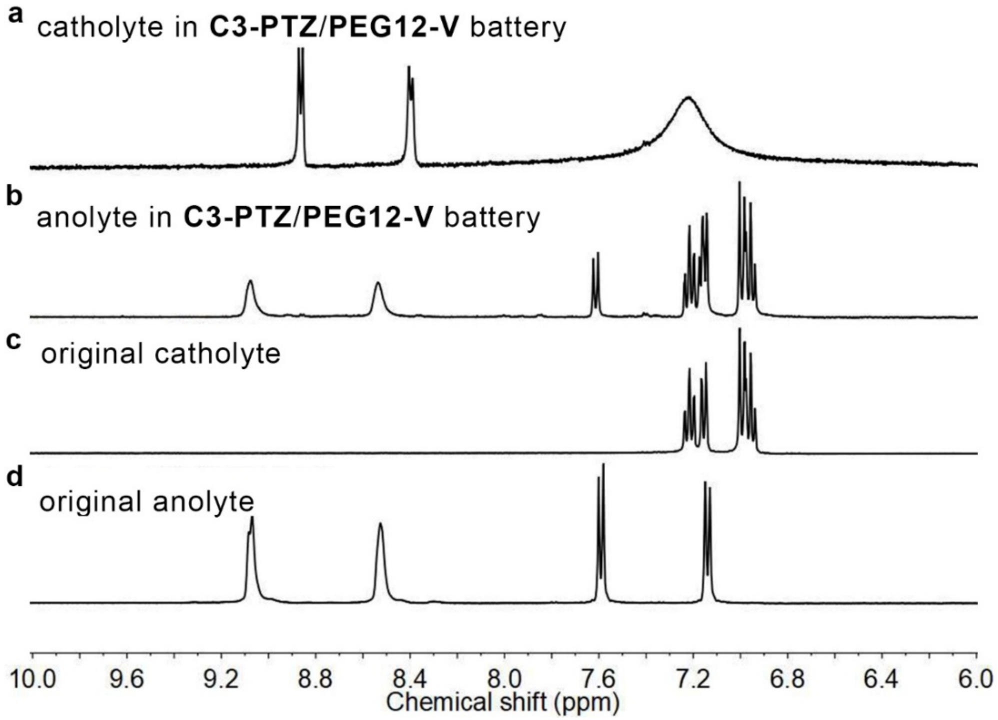

Fig. S14 ^{1}H NMR of catholyte and anolyte in **C3-PTZ/PEG12-V** battery before and after cycling.

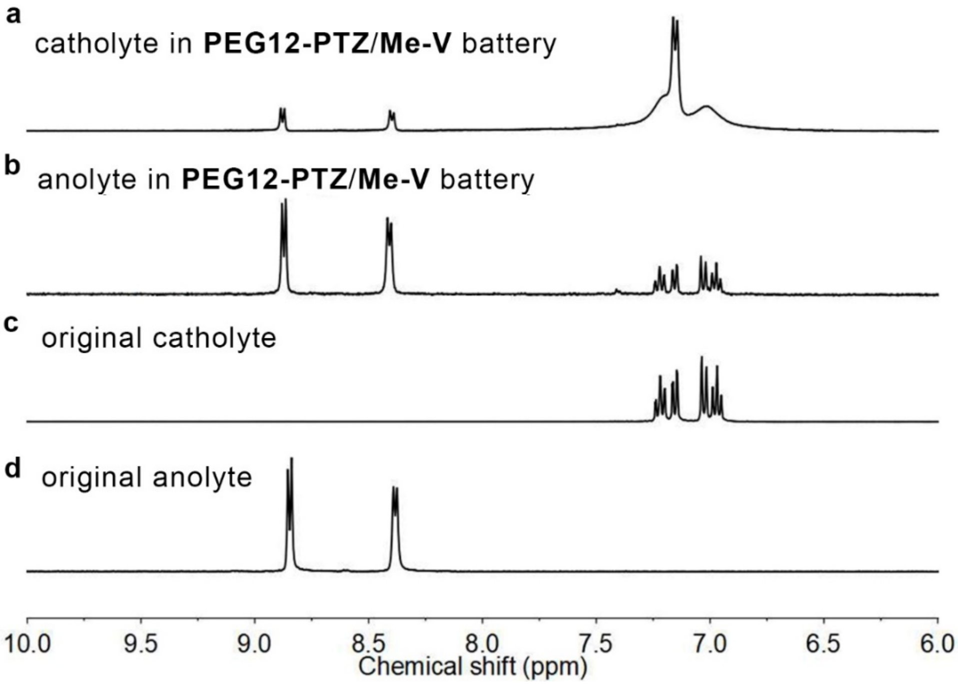

Fig. S15 ^{1}H NMR of catholyte and anolyte in **PEG12-PTZ/Me-V** battery before and after cycling.

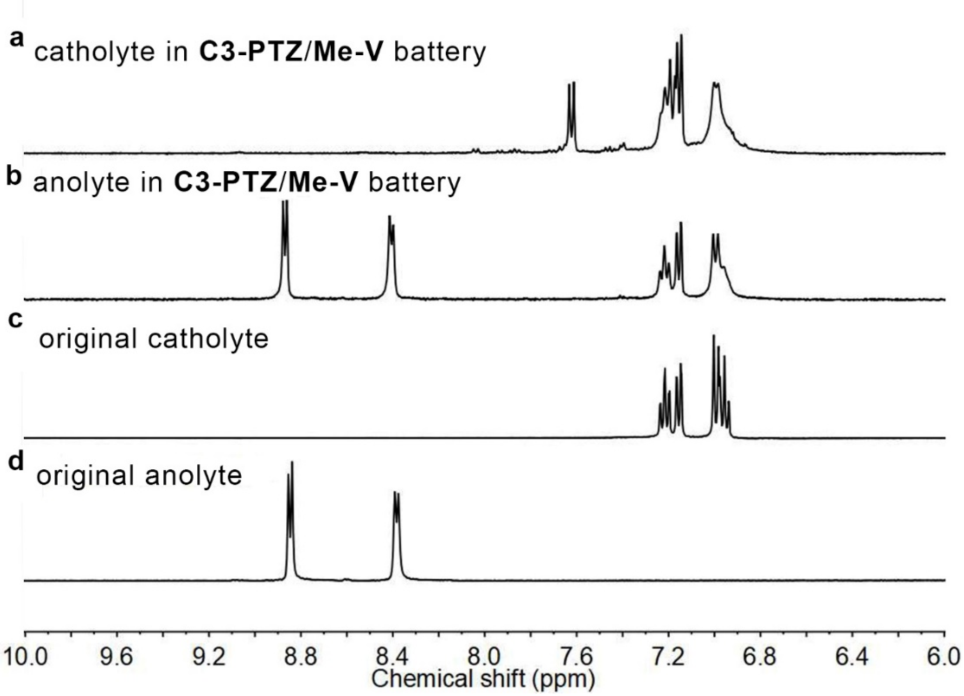

Fig. S16 ^{1}H NMR of catholyte and anolyte in **C3-PTZ/Me-V** battery before and after cycling.

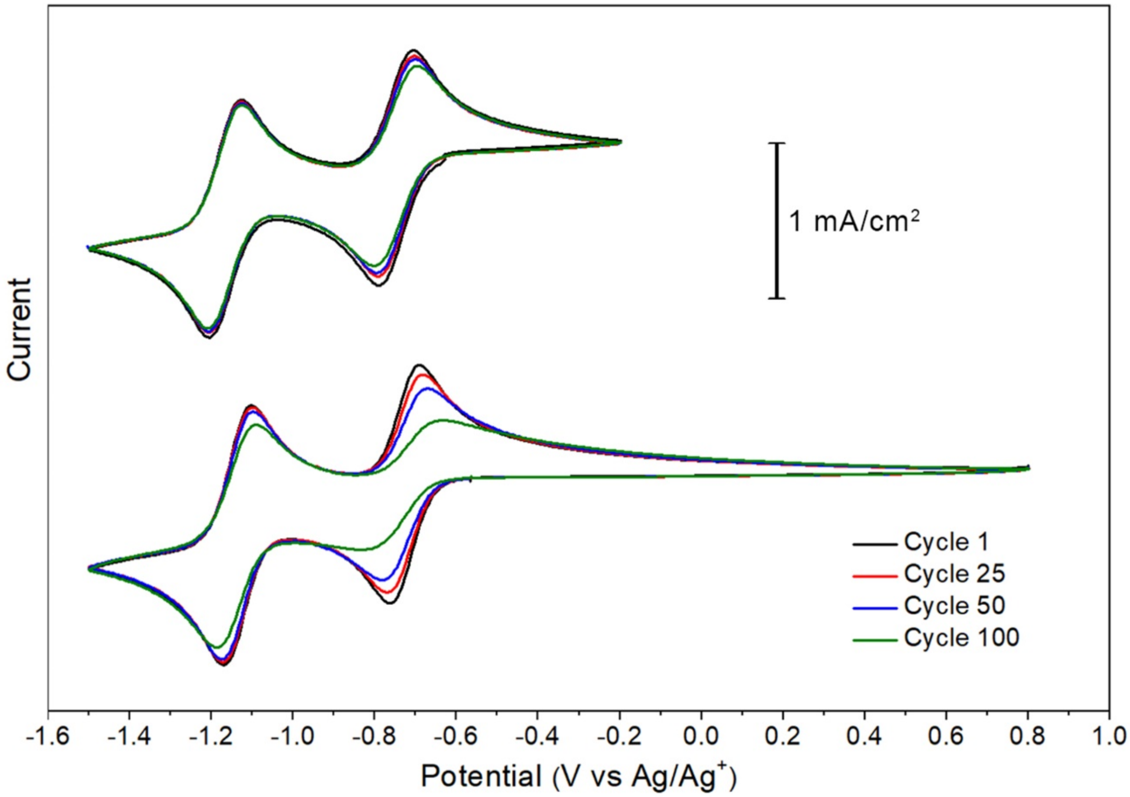

Fig. S17 CV scans of 5 mM **PEG12-V** in 0.1 M $TBAPF_6$-ACN for 100 cycles.

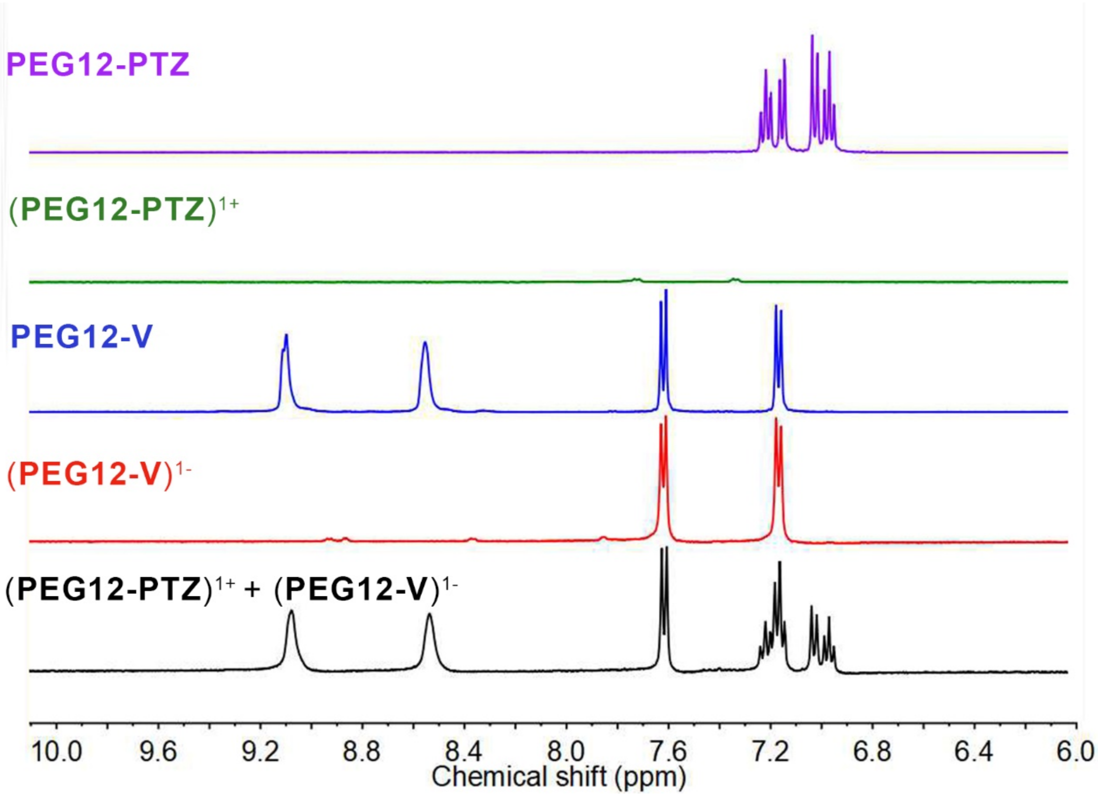

Fig. S18 ^{1}H NMR spectra of **PEG12-PTZ**, (**PEG12-PTZ**)$^{1+}$, **PEG12-V**, (**PEG12-V**)$^{1-}$, and mixture of (**PEG12-PTZ**)$^{1+}$ and (**PEG12-V**)$^{1-}$ in a molar rate of 1:1.

References

S1. Z. J. Yang, L. C. Tong, D. P. Tabor, E. S. Beh, M. A. Goulet, D. De Porcellinis, A. Aspuru-Guzik, R. G. Gordon and M. J. Aziz, *Adv. Energy Mater.*, 2018, **8**, 1702056.

S2. B. Hu and T. L. Liu, *J. Energy Chem.*, 2018, **27**, 1326-1332.

S3. T. Ma, Z. Pan, L. Miao, C. Chen, M. Han, Z. Shang and J. Chen, *Angew. Chem. Int. Ed.*, 2018, **57**, 3158-3162.

S4. K. Lin, R. Gómez-Bombarelli, E. S. Beh, L. Tong, Q. Chen, A. Valle, A. Aspuru-Guzik, M. J. Aziz and R. G. Gordon, *Nat. Energy*, 2016, **1**, 16102.

S5. E. S. Beh, D. De Porcellinis, R. L. Gracia, K. T. Xia, R. G. Gordon and M. J. Aziz, *ACS Energy Lett.*, 2017, **2**, 639-644.

S6. B. Hu, C. DeBruler, Z. Rhodes and T. L. Liu, *J. Am. Chem. Soc.*, 2017, **139**, 1207-1214.